



## International Journal Of Engineering Sciences & Management Research

### PERFORMANCE OF GEOSYNTHETIC-REINFORCED GYPSEOUS SOIL

Hussein H. Karim\*<sup>1</sup>, Zeena W. Samuel<sup>2</sup> & Huda K. Karim<sup>3</sup>

\*<sup>1</sup>Professor, Building and Construction Engineering Department, University of Technology, Baghdad-Iraq

<sup>2</sup>Assistant Professor, Building and Construction Engineering Department, University of Technology, Baghdad-Iraq

<sup>3</sup>M.Sc. in Geotechnical Engineering, Building and Construction Engineering Department, University of Technology, Baghdad-Iraq

**Keywords:** *Gypseous soil, Soil reinforcement, Geogrid, Bearing capacity, Settlement, Foundation*

#### ABSTRACT

As the presence of gypsum in soil affects its engineering properties and behavior in a degree, which is greatly dependent on the amount of gypsum, thus ground improvement and stabilization techniques are needed. The main purpose of the work is to conduct a series of model tests subjected to static vertical load to withstand on the ability of soil stabilization with geosynthetic material by using single and double geogrid layers placed at different locations. For this purpose, a special model test setup was used for such testing. In the light of experimental tests and analyses of these model tests, it is found the settlement ratio of the untreated soil increases linearly with an increase of stress with bearing ratio 0.75 and the mode of failure seems to be local shear failure. A reduction in settlement with high bearing capacity is noticed after using single geogrid layer reinforcement compared with the unreinforced soil. The bearing ratio is increased reaching 0.97 when the single geogrid layer depth increases at an optimal depth equals foundation width (B). At this depth, the bearing improvement ratio (BIR) was 1.29 with settlement reduction ratio of 0.74. Increasing the number of geogrid layers results in a decrease in collapse settlement ratio, increasing in bearing ratio compared to untreated soil. The optimal depths for using double geogrid layers were (2/3) B and B with bearing ratio 1.05. Similar enhanced values are obtained for bearing improvement and settlement reduction ratios (1.41 and 0.65 respectively).

#### INTRODUCTION

Collapsible soils are often unsaturated soils that collapse unexpectedly upon wetting with/without any loading. Gypseous soils are one of these soils, in which the presence of gypsum provides cementation in the form of bonding tightens soil particles together. Such soils are characterized by decreasing strength upon wetting, increasing primary and secondary compression and dissolution in continuously seeping water. In general, gypseous soils are reliable for construction under dry and even under short term flow, but become problematic, collapsible and undergo large settlement under long term flooding with water (Al-Muftay, 1997; Al-Saoudi et al., 2011).

The dissolution of gypsum within the soil mass under wetting and loading conditions leads to one or a combination of several processes such as settlement and collapse. In general, the settlement of gypseous soils is mainly due to the dissolution of the cementing gypsum which is accompanied by the collapse of the soil structure especially in sandy gypseous soils (Karim et al., 2015). Thus the presence of gypsum in soil affects its engineering properties and behavior in a degree, which is greatly dependent on the amount of gypsum in the soil.

Gypseous soils are distributed in many regions in the world particularly in arid and semi-arid areas such as Iraq in which such soils form more than 20% of its total surface area (Nashat, 1990). As the engineering properties of such soils are changed upon wetting causing danger on the structure built on. In the last years, many damages were recorded in some strategic projects in Iraq due to presence of gypseous soils underneath the base of foundation. Investigations proved that most of these projects were constructed on gypsum stratum or soil containing an amount of gypsum. Several cases of structural damages have been recorded in Iraq due to problems related to excessive settlement or loss of strength in these soils, particularly if water is present.

As weak soils are unable to withstand tensile stresses due to their grains arrangement, so such soil underneath foundations become unstable and subject to deformations under loads. Thus, ground improvement and stabilization techniques are needed. A variety of reinforcing materials were used as a geosynthetic-reinforced soil (GRS). Geosynthetics (such as geogrids and geotextile) in reinforced earth applications as ground improvement techniques (Smita and Vishwanath, 2014). Many researchers investigate the behavior of gypseous soils during

## International Journal Of Engineering Sciences & Management Research

improvement and stabilization with such materials either alone or a soil-geosynthetic composite used alongside with other reinforced materials such as stone and sand columns.

Ayadat (1990) was one of the pioneers introduce the encasement for collapsible soil treatment through introducing the geofabric reinforcement to the sand column. An increase in ultimate bearing capacity of the sand column, and an obvious decrease in settlement were observed due to the stiffness of the geotextile used. Later, Ayadat et al. (2008) discussed the failure process of the stone column embedded in collapsible soil after wetting. This study reported that the stone columns have failed to strengthen loose fill that displays collapse behavior through the loss of the lateral confinement of the fill. Karim et al. (2009) improved soft clayey soil using stone columns and dynamic compaction techniques. In comparison with untreated soil. It is found the maximum cumulative settlement improvement ratios were 69% and 178% at applied stress for soil models treated with dynamic compaction and 3 stone columns respectively. Araujo et al. (2009) examined the behavior of sand columns encased with geogrid and geotextile embedded in collapsible fine-grained soil concluding that encasing the sand column increases load capacity and stating the need for satisfactory bearing capacity of the soil at the column base. Hanna and Soliman (2010) achieved an experimental investigation on a strip rigid footing resting on homogeneous and reinforced collapsible soils subjected to inundation simulated to groundwater rise to examine the effect of reinforcement on the footing collapse settlement. An empirical formula was presented to predict the collapse settlement of the strip footing. Hussein (2012) investigated the performance of replacement and geosynthetic reinforcement materials to improve the gypseous soils behavior through experimental manufactured model. Collapse of soil under loads was evaluated for different depths of replacement with dune sand and various layers of reinforcement. The results showed that, the most effective thickness of dune sand associated with a geotextile was at the interface, and found to be almost equal to the width of footing. Al-Obaidy (2016) investigated the possibility of using encased stone columns in ground improvement for Iraqi collapsible soil. It is found that such soils were successfully treated by encased stone columns through increases in the load capacity and reductions in the settlements. Karim et al. (2016a) studied the behavior of sand column stabilized by silica fume embedded in soft soil. The results analysis of the model tests indicated an encouraging improvement in load carrying capacity of the columns and considerable reduction in the settlement compared to the conventional stone columns. Karim et al. (2016b) performed several model tests to improve gypseous soil from Iraq with ordinary (common) and encased stone columns (OSC and ESC) under static loading. The study found an increase in bearing ratio and a reduction in settlement in case of OSC compared to untreated soil as confinement and thus stiffness of the stone is provided by the lateral stress within the weak soil. For ESC, it was concluded that there is slight increase in bearing improvement ratio without any significant effect observed in settlement reduction ratio compared to OSC.

The aim of this study is investigating the ability of soil improvement techniques to stabilize the gypseous soil by using single and double geogrid layers placed at different locations through conducting a series of model tests and evaluating the degree of improvement in the settlement reduction and the bearing capacity of the entire system.

### MATEIALS USED AND SOIL CHARACTERIZATION

#### Soil Used

Samples of disturbed normal gypseous soil brought from Ain Al-Tamur (Karbala, Iraq) was used with 30 % gypsum content. X-ray diffraction analysis for the soil used shows that the predominant minerals are quartz, calcite, feldspar, gypsum and palygorskite. The soil grain size distribution is shown in Figure 1. The physical and chemical properties of this soil are presented in Table 1.

#### Geogrid Used

The geogrid reinforcement used (Figure 2) manufactured by Al-Latifya Factory for Plastic Mesh. Engineering properties of this geogrid material is shown in Table 2.

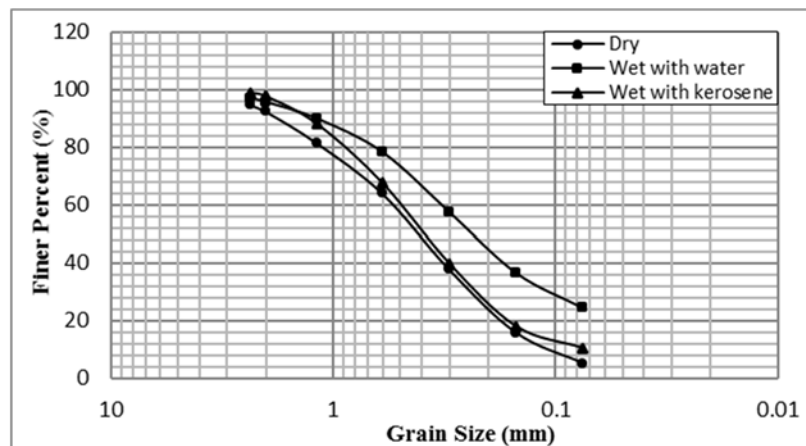


Figure 1 Grain size distribution of the soil used.

Table 1 Physical and chemical properties of the soil used.

| a. Physical Properties                                     |   |       |
|--|---|-------|
| Property   |   | Value |
| Grain size analysis  | Effective size, $D_{10}$ (mm)                                 | 0.11  |
|  | $D_{30}$ (mm)   | 0.24  |
|  | $D_{60}$ (mm)   | 0.55  |
|  | Coefficient of uniformity, ( $C_u$ )                          | 5.0   |
|  | Coefficient of curvature, ( $C_c$ )                           | 0.95  |
|  | Classification (USCS)   | SP    |
| Dry unit weights   | Maximum dry unit weight ( $\text{kN/m}^3$ ), $\gamma_d$ (max) | 14.4  |
|  | Minimum dry unit weight ( $\text{kN/m}^3$ ), $\gamma_d$ (min) | 12.34 |
|  | Test dry unit weight ( $\text{kN/m}^3$ ), $\gamma_d$ (test)   | 12.83 |
|  | Relative density, (R.D %)                                     | 38%   |
| Void ratio   | Maximum void ratio, $e_{\text{max}}$                          | 0.88  |
|  | Minimum void ratio, $e_{\text{min}}$                          | 0.61  |
| Specific gravity, ( $G_s$ )                                |   | 2.32  |
| Initial water content (%)                                  |   | 6     |
| Angle of internal friction before soaking ( $\phi^\circ$ ) |   | 39    |
| Angle of internal friction after soaking ( $\phi^\circ$ )  |   | 27    |
| b. Chemical properties                                     |   |       |
| Gypsum content (%)   |   | 30    |
| Total sulphate content, ( $\text{SO}_3$ %)                 |   | 14    |
| Total soluble salts, (T.S.S %)                             |   | 20.90 |
| pH value   |   | 8.20  |
| X-ray diffraction  | Gypsum, quartz, calcite, feldspar, and palygorskite           |       |



Figure 2 The used geogrid.

Table 2 Engineering properties of geogrid used.

| a. Dimensional properties |             |                  |       |
|---------------------------|-------------|------------------|-------|
| Property                  | Test Method | Unit             | Data  |
| Aperture size             | ISO 9864    | mm × mm          | 6 × 6 |
| Mass per unit area        |             | g/m <sup>2</sup> | 363   |
| Roll width                |             | m                | 1     |
| Roll length               |             | m                | 30    |
| b. Technical properties   |             |                  |       |
| Tensile strength at 2 %   | ISO10319    | kN/m             | 4.3*  |
| Tensile strength at 5 %   |             | kN/m             | 7.7*  |
| Peak tensile strength     |             | kN/m             | 13.5* |
| Yield point elongation    |             | %                | 20.0* |

\*Determined in accordance to Saudi Arabian Standard Organization (SASO) Procedures.

### MODEL TEST SETUP AND METHODOLOGY

Figure 4 displays the formulation of the test setup including the steel frame and axial loading. All models have been inspected using this setup. The dimensions of the soil tank are 60 cm × 60 cm × 75 cm with steel plate thickness of 6 mm (Figure 4). The soil tank model is placed below the steel loading frame with the axial loading system to transfer load (Figure 4a). A rigid square steel base plate with dimensions of 200 mm × 200 mm × 10 mm was used to model footing placed on the model to transfer the load. To record the amount of applied load, a very sensitive digital weighting indicator was used, while a stainless steel compression load cell was used measure load within soil. Loading procedure for testing the models with full details is illustrated in Figure 4b.



Figure 4 (a) Steel frame and axial loading; (b) Full model details.

### Preparation the Bed of Soil

At first, the preparation of the soil bed include three processes, crushing, remixing and air-drying. Then, the required weight of natural soil was mixed with specific amount of water depending on the wet density. A filter material (5 cm in height) was placed at the base of the container which was compacted by a certain hammer to obtain the required density of 13.6 kN/m<sup>3</sup> that gives a relative density of the soil 38 %. A mesh is placed over the filter to prevent mixing with the soil bed. The prepared soil was spread into sublayers (5 cm thick for each), and compacted uniformly to attain the desired density as possible. The soil surface is leveled to get a flat plane. Then,

## International Journal Of Engineering Sciences & Management Research

the model tank is soaked with water for approximately five days. The process of soaking involves lifting water from the base of the tank to the top of soil surface and then lowering the water again to the base of the filter material. Finally, the container is covered with a sheet of nylon to maintain constant water content of soil as possible. Figure 5 illustrates the steps of soil bed preparation.

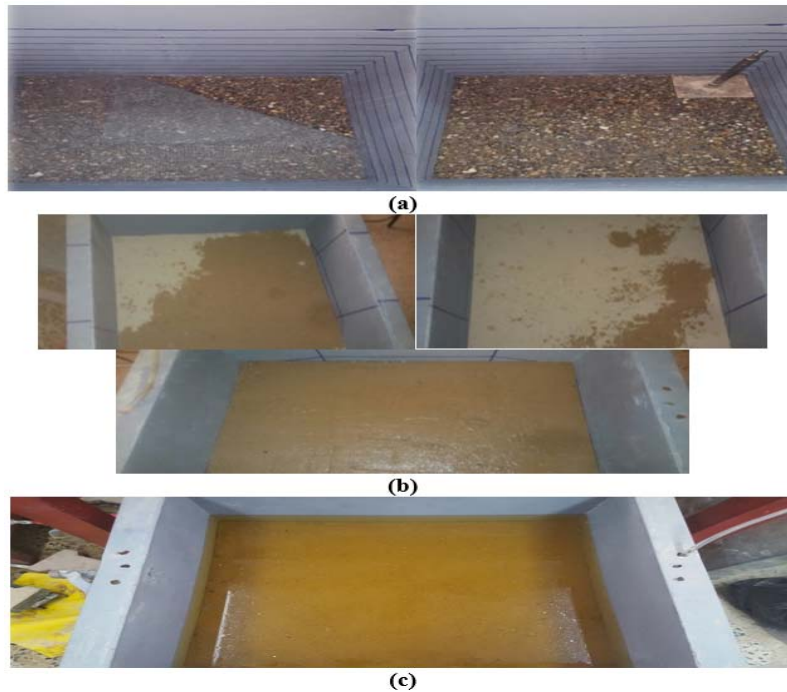


Figure 5 Preparation of soil bed: (a) Placing filter and soil (b) Lifting water for wetting (c) Inundation process.

### Reinforcement of native soil by geogrid

This method is concerned with reinforcing the natural soil using geogrid. The concept of this method depends on placing layers of geogrid beneath the active zone of foundation using single or double layers for each case distributed at certain distances (depths). The dimensions of the geogrid are (55×55) cm, and were placed in horizontal plane. The depths of geogrid layers were chosen to be (1/3) B, (2/3) B, and B for the case of one layer. While different configuration for two layer case of geogrid were used, the depths of these layers were chosen to be (1/3) B and (2/3) B; (1/3) B and B; (2/3) B and B. The procedure of grid installation and locations is illustrated in Figure 6.

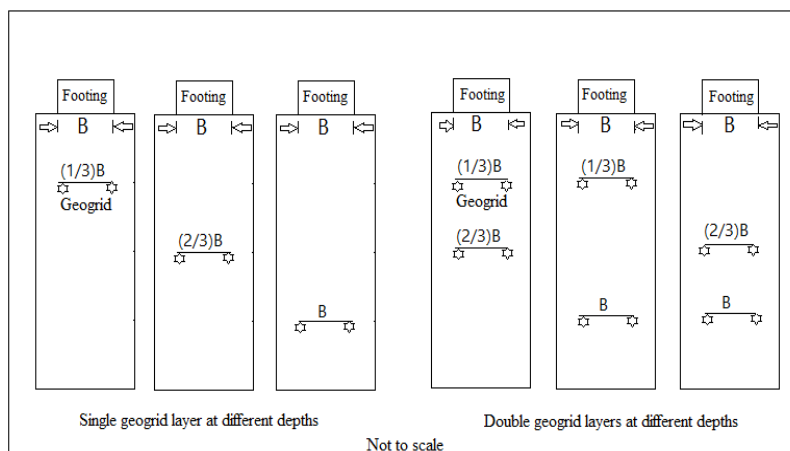


Figure 6 Installation process and locations (depths) of the reinforced geogrid.

# International Journal Of Engineering Sciences & Management Research

## RESULTS AND DISCUSSION

### Untreated Model

One of the model test was performed on a bed of saturated gypseous soil. The footing was placed on the surface of the bed of soil and loaded gradually up to failure. The results of bearing ratio ( $q_u/\gamma B$ ) versus settlement ratio ( $S/B$ ) % are illustrated in Figure 7. It is obvious from this figure that the settlement ratio increases linearly with an increase of stress. The mode of failure seems to be local shear failure. This behavior was expected, where the increase in load would increase the rate of gypsum solution and cause softening of the soil resulting in loss of shear strength and increase in collapse settlement. The obtained ultimate bearing capacity ratio is 0.78.

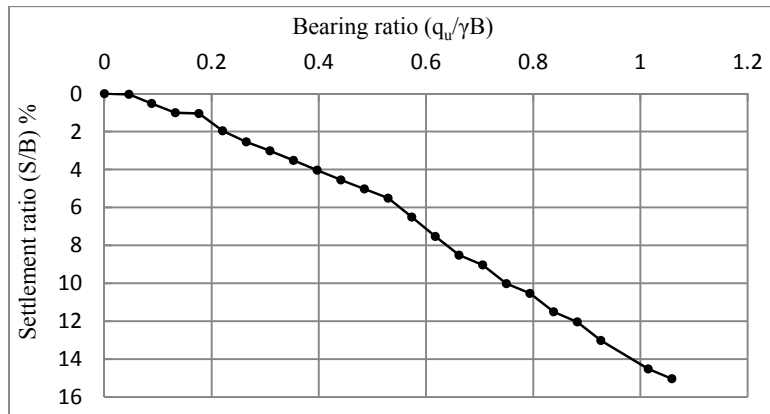


Figure 7 Settlement ratio versus bearing ratio for a footing resting on untreated gypseous soil.

### Model Tests on Treated Gypseous Soil

#### Model tests on native soil reinforced by using single geogrid layer

Three model tests were carried out by reinforcing the gypseous soil with single geogrid layer placed at depths of  $(1/3) B$ ,  $(2/3) B$ , and  $B$ .

#### Bearing ratio versus settlement ratio

Figure 8 shows the relationship between the bearing ratio ( $q_u/\gamma B$ ) and settlement ratio ( $S/B$ ) % for the case of native soil reinforced by a single geogrid layer overlaying the bed of gypseous soil. Reduction in settlement with high growing in bearing capacity is noticed after reinforcement when compared with the unreinforced gypseous soil. It can be also noticed that the best depth which gives the minimum collapse settlement and high bearing ratio when the geogrid layer is placed at depth of  $B$  as confirmed by Hussein (2012). This behavior was expected due to an increase in the dissolution of gypsum. Figure 9 illustrates the relationship between the distance (depth) of geogrid layer and bearing ratio ( $q_u/\gamma B$ ) at failure. The figure indicates that the bearing ratio at failure is increased when the geogrid layer depth increases. The maximum bearing ratio at failure was observed at depth  $B$  below footing. The values of bearing ratio at failure are summarized in Table 3.

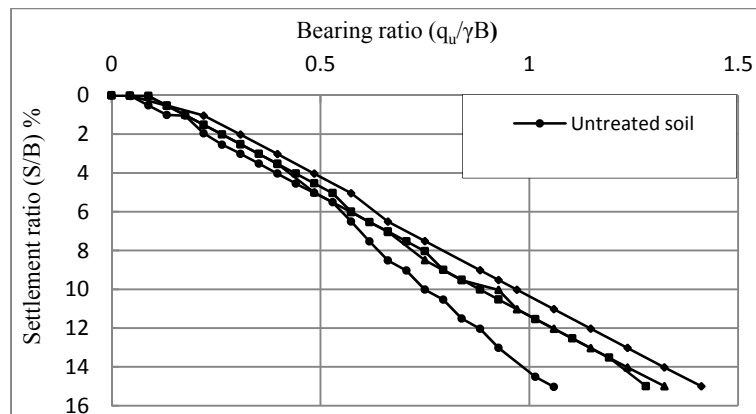


Figure 8 Settlement ratio versus bearing ratio for a footing resting on native soil reinforced by single geogrid layer.

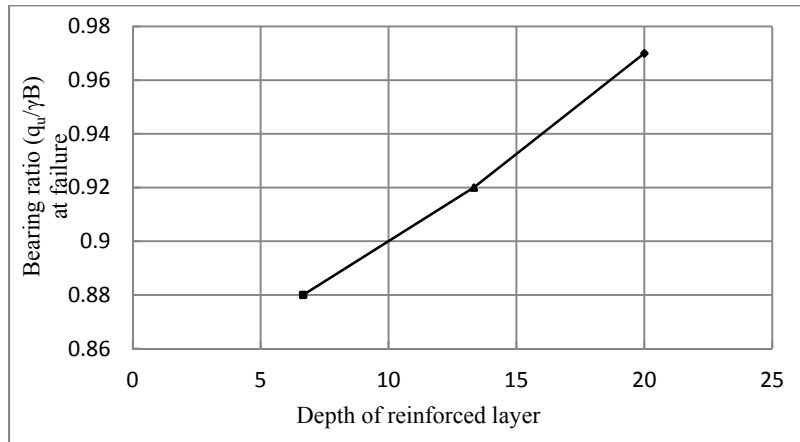


Figure 9 Bearing ratio at failure versus the location (depth) of single geogrid layer.

Table 3 Values of bearing capacity ratio ( $q_u/\gamma B$ ), bearing improvement ratio ( $q_t/q_{unt}$ ) and settlement reduction ratio ( $S_t/S_{unt}$ ) at failure for native soil reinforced by using single geogrid layer.

| Case  | $q_u/\gamma B$ | $q_t/q_{unt}$ | $S_t/S_{unt}$ |
|---|----------------|---------------|---------------|
| Untreated soil  | 0.75           | -             | -             |
| Reinforcement of native soil by single geogrid layer at depth (1/3) B | 0.88           | 1.17          | 0.75          |
| Reinforcement of native soil by single geogrid layer at depth (2/3) B | 0.92           | 1.23          | 0.81          |
| Reinforcement of native soil by single geogrid layer at depth B       | 0.97           | 1.29          | 0.74          |

**Bearing improvement ratio versus settlement ratio**

To evaluate the amount of settlement reduction ratio achieved by the geogrid reinforcement, a bearing improvement ratio is introduced which represents the ratio of  $(q/\gamma B)_t$  for the treated soil divided by the corresponding  $(q/\gamma B)_{unt}$  for the untreated soil. The variation of bearing improvement ratio ( $q_t/q_{unt}$ ) at failure versus settlement ratio (S/B) % for native soil reinforced by single geogrid layer is shown in Figure 10. It can be seen that there is a consistent increase in bearing improvement ratio (BIR) versus settlement ratio (S/B) %. Peaks values of improvement ratio are observed at nearly S/B=0.52, 0.51 and 0.51% respectively, then drops down and remains nearly constant with increasing settlement ratio. This behavior is due to the fact that the reinforcement of native soil by single geogrid layer is stiffer than the surrounding soil. Figure 11 shows the relationship between the depth of geogrid layer and bearing improvement ratio ( $q_t/q_{unt}$ ). The two figures indicate a general increase trend, however, approximate linear increasing trend is observed. The bearing improvement ratio values at failure for different locations of single geogrid layer are also shown in Table 3. This table indicates that the BIR at failure is increased when the geogrid layer was placed at depth of B below footing which was equal to 1.29.

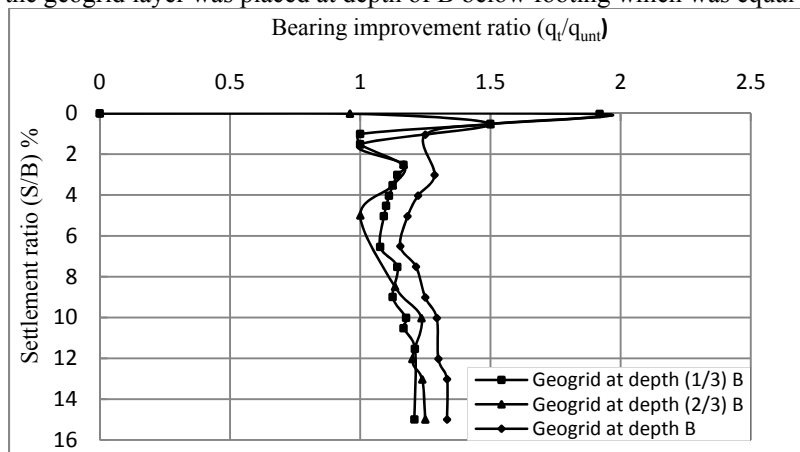


Figure 10 Settlement ratio versus bearing improvement ratio for a footing resting on native soil reinforced by single geogrid layer.

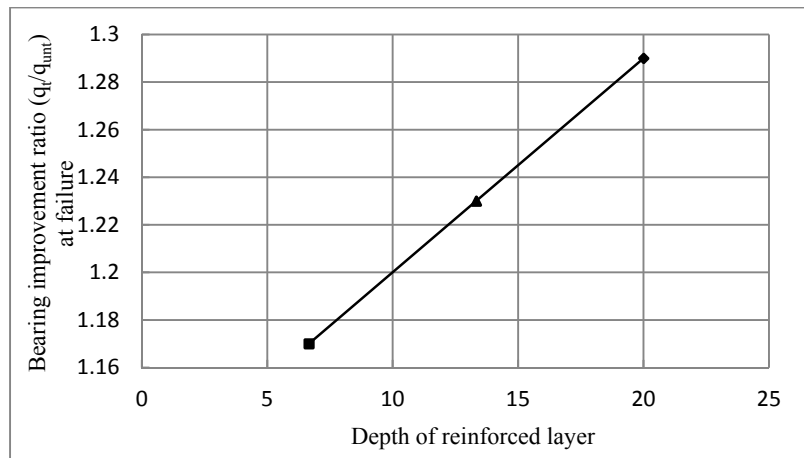


Figure 11 Bearing improvement ratio at failure versus depth of single geogrid layer.

### Settlement reduction ratio versus bearing ratio

Different settlement reduction ratios ( $S_t/S_{unt}$ ) versus bearing ratios ( $q_u/\gamma B$ ) with reinforcement of native soil by single geogrid layer are displayed in Figure 12. Since the failure was defined as the applied stress that corresponds to ( $S/B=10\%$ ), then the settlement reduction ratio was determined as ( $S_t/S_{unt}$ ) where  $S_{unt}$  represents a settlement at a constant value of 10% of the footing diameter for the untreated soil. The  $S_t$  represents the settlement of the treated soil corresponding to the failure pressure of the untreated model. The results reveal a decrease in settlement reduction ratio. From examining the results, it is observed that the best reduction in collapse settlement ratios was noticed when using one geogrid layer at depth equals  $B$ . While, lower settlement reduction ratio was noticed at a depth of  $(2/3)B$ . Figure 13 demonstrates the relationship between the depth of geogrid layer and settlement reduction ratio ( $S_t/S_{unt}$ ). Results of the settlement reduction ratio at failure ( $S_t/S_{unt}$ ) for the case of native soil reinforced by single geogrid layer are presented in Table 3.

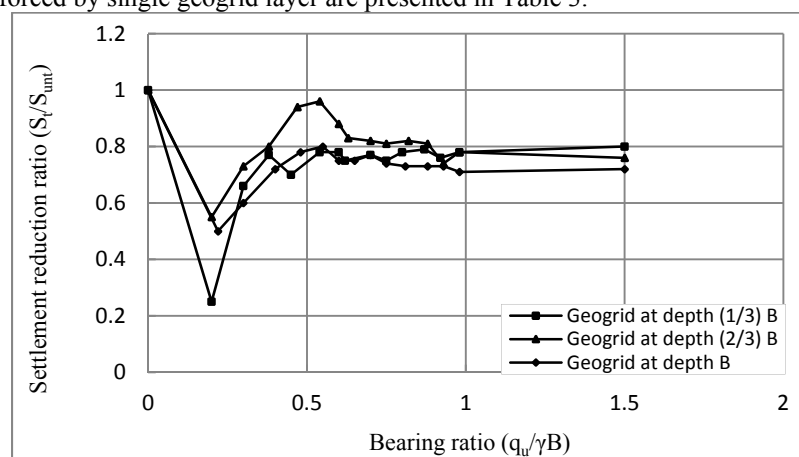


Figure 12 Settlement reduction ratio versus bearing ratio for a footing resting native soil reinforced by single geogrid layer.



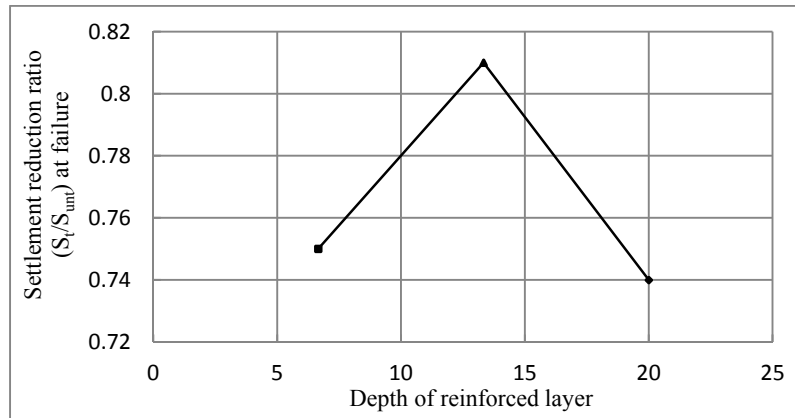


Figure 13 Settlement reduction ratio at failure versus depth of single geogrid layer.

**Model tests on native soil reinforced by double geogrid layers**

Three model tests were performed on native soil reinforced by double geogrid layers. The depths of these layers were chosen to be (1/3) B and (2/3) B; (1/3) B and B; (2/3) B and B for the case of two geogrid layers.

**Bearing ratio versus settlement ratio**

Figure 14 represents the relationship between the bearing ratio ( $q_u/\gamma B$ ) and settlement ratio ( $S/B$ ) % for the case of native soil reinforced by double geogrid layers. It can be seen that an increasing in the number of geogrid layers results in a decrease in collapse settlement ratio, and increasing in the bearing ratio ( $q_u/\gamma B$ ) with increasing number of reinforcing layers as compared with the case of untreated soil. This behavior may be attributed to the high resistance between the reinforcement and soil particles. The geogrid reinforcements perform the increase in stiffness where the horizontal shear strains and vertical settlement are controlled and minimized. The result values of the bearing ratio at failure are summarized in Table 4. The table indicates that the bearing ratio at failure is increased with increasing number of geogrid layers due to the interaction between each other.

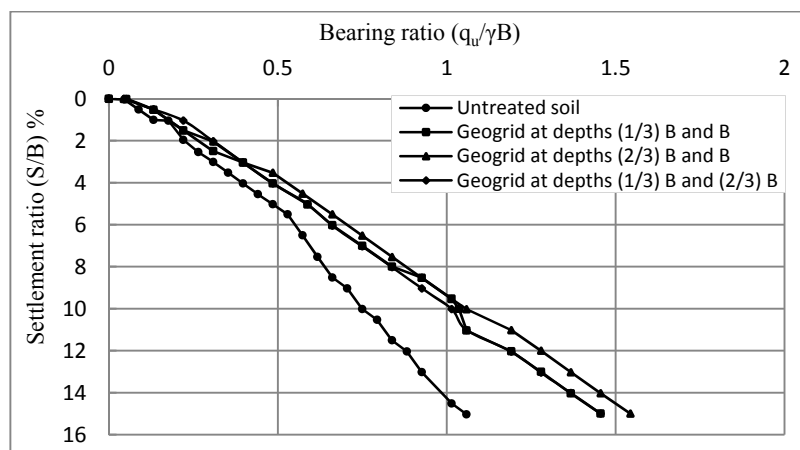


Figure 14 Settlement ratio versus bearing ratio for a footing resting on native soil reinforced by double geogrid layers.

Figure 15 shows the relationship between the depth of double geogrid layers and bearing ratio ( $q_u/\gamma B$ ). The figure indicates an increasing trend in bearing ratio (BR) at failure with increasing number of geogrid layer. Maximum values were obtained when geogrid at depths (2/3) B and (1/3) B.

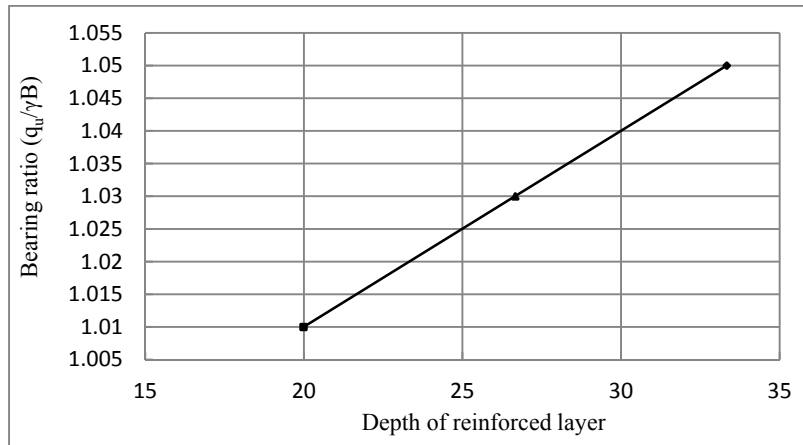


Figure 15 Relationship between the bearing ratio ( $q_u/\gamma B$ ) and the settlement ratio (S/B) %.

Results of untreated soil, soil reinforced by single geogrid layer at depths (1/3) B; (2/3) B and B respectively and soil reinforced by double geogrid layers at depths (1/3) B and (2/3) B; (1/3) B and B; and (2/3) B and B respectively are also presented in Figure 16 for comparison purposes.

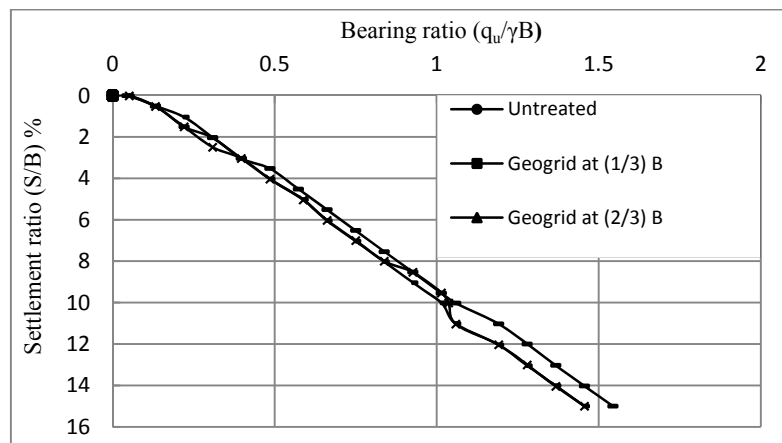


Figure 16 Settlement ratio versus bearing ratio for a footing resting on native soil reinforced by single and double geogrid layers.

**Bearing improvement ratio versus settlement ratio**

The variation of bearing improvement ratio ( $q_t/q_{unt}$ ) versus settlement ratio (S/B) % for soil treated with double geogrid layer at different configurations is shown in Figure 17. The figure show peaks values of improvement ratio observed at S/B= 0.51, 0.52 and 0.52 % respectively followed by a sudden drop, and then remains nearly constant with increase in deformation ratio. Figure 18 illustrates the relationship between the depth of double geogrid layer and bearing improvement ratio( $q_t/q_{unt}$ ) at failure.

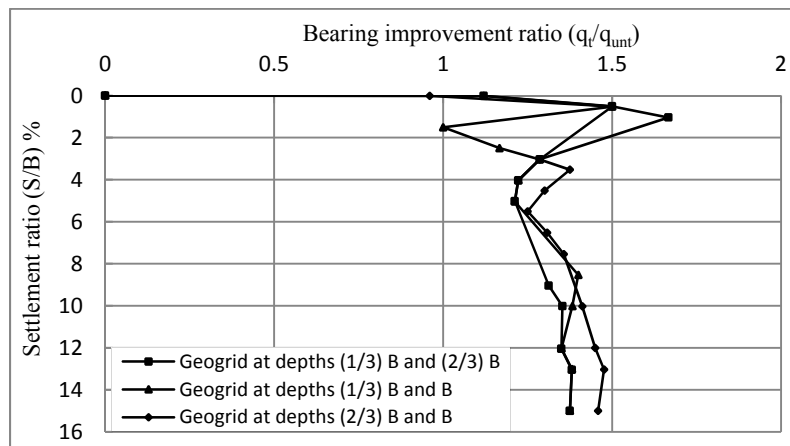


Figure 17 Settlement ratio versus bearing improvement ratio for a footing resting on native soil reinforced by double geogrid layer.

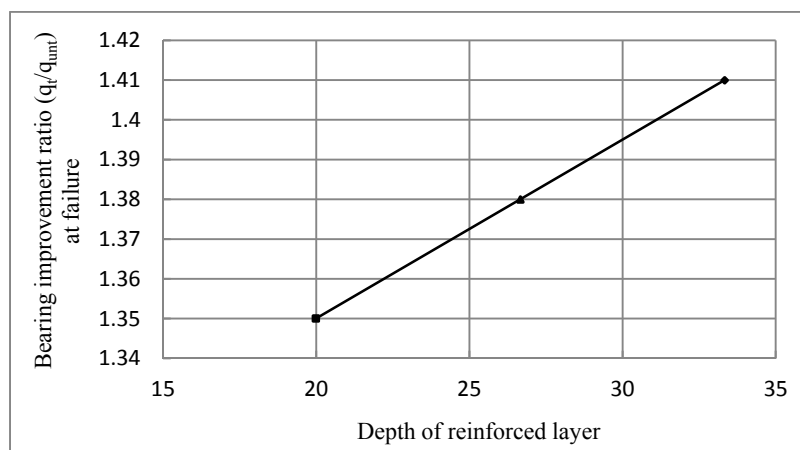


Figure 18 Bearing improvement ratio at failure versus depth of double geogrid layer.

The values of bearing improvement ratio at failure, presented in Table 4, indicates that the bearing improvement ratio at failure is increased with increasing number of geogrid layers due to the interaction between each other.

Table 4 Values of bearing capacity ratio ( $q_u/\gamma B$ ), bearing improvement ratio ( $q_t/q_{unt}$ ) and settlement reduction ratio ( $S_t/S_{unt}$ ) at failure for native soil reinforced by double geogrid layers.

| Case   | $q_u/\gamma B$ | $q_t/q_{unt}$ | $S_t/S_{unt}$ |
|--|----------------|---------------|---------------|
| Untreated  | 0.75           | -             | -             |
| Reinforcement of native soil with double geogrid layers at (1/3) B and (2/3) B | 1.01           | 1.35          | 0.67          |
| Reinforcement of native soil with double geogrid layers at (1/3) B and B       | 1.03           | 1.38          | 0.67          |
| Reinforcement of native soil with double geogrid layers at (2/3) B and B       | 1.05           | 1.41          | 0.65          |

**Settlement Reduction Ratio versus Bearing Ratio**

Different settlement reduction ratios ( $S_t/S_{unt}$ ) versus bearing ratio ( $q_u/\gamma B$ ) with reinforcement of native soil by double geogrid layers are shown in Figure 19. It can be seen that a decrease in collapse settlement ratio with increasing number of geogrid layers. This behavior may be attributed to the high friction resistance between the soil particles and reinforcement as noticed by Hussein (2012). Figure 20 shows the relationship between the depth of double geogrid layers and settlement reduction ratio ( $S_t/S_{unt}$ ). The values of the settlement reduction ratio at failure ( $S_t/S_{unt}$ ) for reinforcement cases of native soil by double geogrid (Table 4) reflect that the native soil reinforced by double geogrid layer at depth (2/3) B and B provided the optimal results.

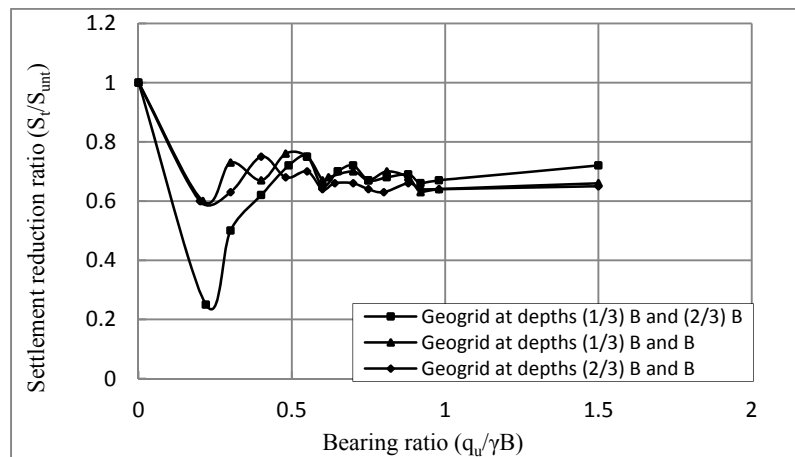


Figure 19 Settlement reduction ratio versus bearing ratio for soil treated with reinforcement of native soil by double geogrid layer.

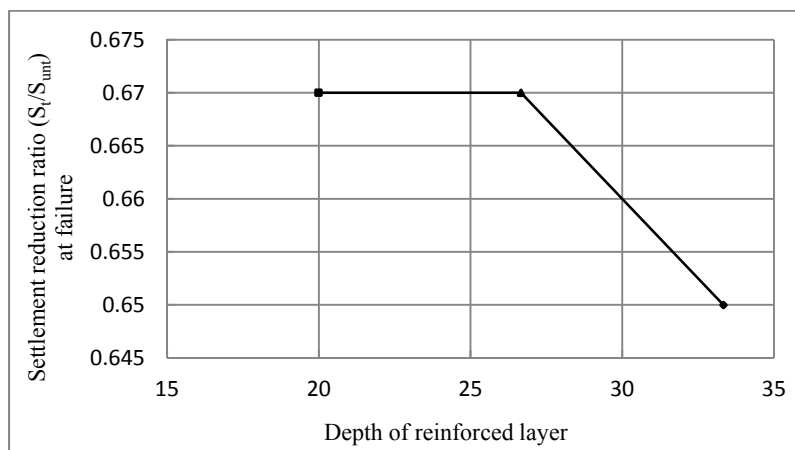


Figure 20 Settlement reduction ratio at failure versus depth of double geogrid layer.

## CONCLUSIONS

On the light of experimental tests and analyses of model tests performed on unreinforced and reinforced soils using single and double geogrid layers under static loading, the following conclusions can be drawn:

1. For untreated soil, the settlement ratio increases linearly with an increase of stress and the mode of failure seems to be local shear failure.
2. The bearing ratio is increased from 0.75 for untreated soil to 0.97 for soil reinforced by single geogrid layer at depth equals footing width (B).
3. The bearing ratio is increased when the geogrid layer depth increases. The best depth gives minimum collapse settlement with high bearing ratio when single geogrid layer is placed at depth of B below footing with BIR equals 1.29.
4. Increasing the number of geogrid layers results in a decrease in collapse settlement ratio, and increasing in the bearing ratio (1.05) as compared with the case of untreated soil.

The bearing improvement ratio (BIR) increases to and 1.41 for soil reinforced by double geogrid layers at depths (2/3) B and B. These depths provided the optimal results as maximum bearing, bearing improvement, and settlement reduction ratios are obtained.

## REFERENCES

1. Al-Mufti, A. A., *Effect of gypsum dissolution on the mechanical behaviour of gypseous soils*, Ph.D thesis, Civil Eng. Dep., University of Baghdad, Baghdad, Iraq, 1997.
2. Al-Obaidy, N., Jefferson, I., and Ghataora, G., *Treatment of Iraqi collapsible soil using encased stone columns*, The 15th Asian Regional Conference on Soil Mechanics and Geotechnical Engineering,



## International Journal OF Engineering Sciences & Management Research

*Japanese Geotechnical Society Special Publication, pp.564-569, Article - January 2016, DOI: 10.3208/jgssp.IRQ-01, <http://doi.org/10.3208/jgssp.IRQ-01>, 2016.*

3. Al-Saoudi, N. K. S. Al-Nouri I. M. A., Sheikha A. A. H., *The collapsible behavior of gypseous soils, Jordanian Geologists Association, the 7th Jordanian Geological Conference, 2011.*
4. Araujo, G., Palmeira, E., and Cunha, R., *Behaviour of geosynthetic-encased granular columns in porous collapsible soil, Geosynthetics International, 16(6), 2009, pp.433–451.*
5. Ayadat, T., *Collapse of stone column foundations due to inundation. PhD thesis, University of Sheffield, 1990.*
6. Ayadat, T., Hanna, A. and Etezzad, M., *Failure process of stone columns in collapsible soils, IJE Transactions B: Applications, 21(2), 2008, pp.135–142.*
7. Hanna, A., and Soliman, S., *Performance of reinforced collapsible soil, Advances in Analysis Modeling and Design, ASCE, 2010, pp. 347-356.*
8. Hussein, R. S., *Bearing capacity of shallow footing on compacted dune sand over reinforced gypseous soil, M.Sc. Thesis, University of Baghdad, Iraq, 2012.*
9. Karim, H.H., Mahmood, M. M. and Renka, R. G., *Soft clay soil improvement using stone columns and dynamic compaction techniques. Eng. & Technology Jour., Uni. of Technology. 27(14), 2009, pp.2546-2565.*
10. Karim, H. H., Schanz, T. and Ibrahim, A. N., *Microstructural Characterization of Iraqi Gypseous Soils. Proceedings of the 2nd International Conference of Buildings, Construction and Environmental Engineering, American University of Beirut (BCEE2), 17-18 Oct., 2015. Geotechnical Engineering part, 2015, pp. 95-100.*
11. Karim, H. H., Samueel, Z. W. and Mohammed, M. S., *Sand Column Stabilized by Silica Fume Embedded in Soft Soil, Eng. & Technology Jour., Vol. 34 (A), No. 6, 2016a, pp.1047-1057.*
12. Karim, H. H., Samueel, Z.W. and Karim H.K., *Iraqi gypseous soil stabilized by ordinary and encased stone columns, International Journal of Civil Engineering and Technology, 7(6), 2016b, pp.179 – 192.*
13. Nashat, I. H., *Engineering characteristics of some gypseous soils in Iraq, Ph.D thesis, Civil Eng. Dep., University of Baghdad, Baghdad, Iraq, 1990.*
14. Smita G.M, and Vishwanath C.S., *Strengthening of expansive soil to reduce settlement, International Journal of Research in Engineering and Technology (IJRET), 03(03), Special Issue, NERIET-2014, pp.617-622, 2014, Available @ <http://www.ijret.org>*